

---

# Deep Overcomplete Tensor Rank-Decompositions

---

**Andrew Stevens**  
Duke Univ. & PNNL  
ajs104@duke.edu

**Yunchen Pu**  
Duke Univ.

**Yannan Sun**  
PNNL

**Gregory Spell**  
Duke Univ.

**Lawrence Carin**  
Duke Univ.

## Abstract

We introduce new dictionary learning methods for tensor-variate data. Our model need not be separable and we infer the tensor-rank of each dictionary atom. This is possible through the novel combination and extension of beta-process factor analysis (BPFA) and the multiplicative gamma process CANDECOMP/PARAFAC (MGP-CP). We also extend our tensor factor analysis (TFA) model to a deep convolutional setting. We test our approach on image processing and classification tasks achieving state of the art results for inpainting and Caltech 101. The experiments also show that atom-rank impacts overcompleteness and sparsity.

## 1 Introduction

The first data analysis applications of tensors saw the development of the Tucker and canonical decomposition (CANDECOMP) in chemometrics and the parallel factor model (PARAFAC) in linguistics [1]. The Tucker decomposition has been more recently named the multilinear or high-order singular value decomposition (HOSVD) [2]. Most recently, tensor methods have been applied in signal/image processing and machine learning [1].

The focus of this paper is overcomplete dictionary learning. We are especially interested in tensor-variate data and tensor-variate dictionary atoms/elements (or factor loadings). An overview of non-tensor dictionary learning approaches can be found in [3]. The goal of overcomplete dictionary learning is to find a set of atoms that can represent a data item as a weighted sum of a small subset of those atoms. A dictionary is called overcomplete when the number of atoms  $K$  is greater than the number of elements  $P$  of each data item, this is closely related frame theory [4]. Overcompleteness is desirable because it offers robustness to noise, increased sparsity, and improved interpretability [5].

The concept of overcompleteness becomes unclear when we move to high-order data. Vectors can be represented as a sum of basis elements, so an overcomplete dictionary gives us more elements than we need to represent a vector. Matrices (2-way tensors) can be represented as either a sum of basis elements (a flat representation) or as a sum of rank-1 matrices (SVD). If a particular matrix is  $m_1 \times m_2$ , we need more than  $m_1 m_2$  atoms for overcompleteness, whereas a rank-decomposition only needs more than  $\min\{m_1, m_2\}$ —we call this rank-overcomplete.

Previous work in overcomplete tensor-dictionary learning has focused on separable models [6–8]. Imposing separable structure means that each atom is a rank-1 tensor. Moreover, they consider only “shallow” representations. This paper makes the following contributions: 1) an overcomplete tensor representation with atoms of arbitrary rank and data of any order—our representation is a natural extension of dictionary learning and allows non-separable dictionaries; 2) a method to learn the shrinkage rate for the singular values of each atom, which manages model complexity during learning and extends an existing CANDECOMP/PARAFAC algorithm; 3) an online learning approach that produces comparable results to Gibbs sampling with a very few iterations through the whole data set; 4) extensions of our model for convolutional and deep learning; 5) experimental results on image processing and classification tasks with state of the art results for inpainting and Caltech 101, and evidence that rank is an important aspect of sparse-overcomplete modeling.

## 2 Preliminaries

**Dictionary learning:** Formally, dictionary learning is a factorization of a data tensor  $\mathcal{X}$ . If the data are column vectors we have  $\mathbf{X} = \mathbf{D}\mathbf{W} + \mathbf{E}$ , where the  $N$  data vectors are combined into the matrix  $\mathbf{X} \in \mathbb{R}^{P \times N}$ , the dictionary  $\mathbf{D} \in \mathbb{R}^{P \times K}$ , the weight matrix  $\mathbf{W} \in \mathbb{R}^{K \times N}$ , and  $\mathbf{E}$  is the residual/noise. When  $K > P$  it is necessary to impose that  $\mathbf{W}$  is sparse to ensure identifiability.

Beta-process factor analysis (BPFA) is a Bayesian nonparametric model for dictionary learning [9]. In BPFA we assume that the noise is Gaussian and impose sparsity using a truncated beta-Bernoulli process [9]. The BPFA model is specified as

$$\begin{aligned} \mathbf{x}_n &\sim \mathcal{N}(\mathbf{D}\mathbf{w}_n, \gamma_\epsilon^{-1}\mathbf{I}_P), & \mathbf{d}_k &\sim \mathcal{N}(0, P^{-1}\mathbf{I}_P), & \mathbf{w}_n &= \mathbf{s}_n \circ \mathbf{z}_n \\ \mathbf{s}_n &\sim \mathcal{N}(0, \gamma_s^{-1}\mathbf{I}_K), & z_{kn} &\sim \text{Bernoulli}(\pi_k), & \pi_k &\sim \text{Beta}(a_\pi/K, b_\pi(K-1)/K), \end{aligned} \quad (1)$$

where  $\gamma_\epsilon, \gamma_s$  have noninformative gamma priors with all hyperparameters set to  $10^{-6}$ , the prior for  $\pi_k$  is nearly uniform with  $a_\pi = K$ ,  $b_\pi = 1$ , and  $\circ$  is the Hadamard elementwise product. The probabilities  $\pi_k$  determine how likely an atom is to be used—the hyperparameters directly affect sparsity. Other priors for the weights have been proposed in [10–13]. A Gaussian process construction for the dictionary is given in [14].

**Tensor decomposition:** A tensor is a mathematical object describing linear transformation rules, and once we fix a basis we can represent a tensor as a multidimensional array of numbers. In data analysis, it is common to call a multidimensional array a tensor. An entry of a  $T$ -way or order- $T$  tensor  $\mathcal{X} \in \mathbb{R}^{m_1 \times \dots \times m_T}$  is indicated by a position vector  $\mathbf{i} = [i_1, \dots, i_T]$ , where  $i_t$  is an integer on  $[1, m_t]$ ; we denote the  $i^{\text{th}}$  entry of the tensor  $\mathcal{X}$  as  $x_i$ . We use  $\otimes$  to represent both the Kronecker product and the tensor outer product—it will be clear from the context which is being used. The two products are isomorphic; the Kronecker product is a matricization of the tensor outer product. We also use the mapping  $\mathbf{x} = \text{vec}(\mathcal{X})$ , defined by  $x_i = \text{vec}(\mathcal{X})_{i_1+i_2m_1+\dots+i_Tm_1 \dots m_{T-1}}$ .

If we consider a matrix  $\mathbf{X} \in \mathbb{R}^{m_1 \times m_2}$  we can write it as  $\mathbf{X} = \sum_{r=1}^{m_1 \wedge m_2} \lambda_r \mathbf{u}_r^{(1)} \mathbf{u}_r^{(2)\top}$ , where  $\lambda_r \in \mathbb{R}$ ,  $\mathbf{u}_r^{(1)} \in \mathbb{R}^{m_1}$ ,  $\mathbf{u}_r^{(2)} \in \mathbb{R}^{m_2}$ . This is the SVD. A generalization of the SVD to a  $T$ -way tensor  $\mathcal{X}$  is called the canonical polyadic decomposition (PD). The canonical PD is written as  $\mathcal{X} = \sum_{r=1}^{R_M} \lambda_r \otimes_{t=1}^T \mathbf{u}_r^{(t)}$ , where  $R_M$  is the maximum rank of tensors in  $\mathbb{R}^{m_1 \times \dots \times m_T}$ ,  $\mathbf{u}_r^{(t)} \in \mathbb{R}^{m_t}$ . The rank of a particular tensor is the number of nonzero  $\lambda_r$ . The maximum rank  $R_M$  is usually not  $\min_t m_t$  like the matrix case. A tensor is called unbalanced when  $m_T \geq 1 + \prod_{t=1}^{T-1} m_t - \sum_{t=1}^{T-1} (m_t - 1)$  and balanced when  $m_T \leq \prod_{t=1}^{T-1} m_t - \sum_{t=1}^{T-1} (m_t - 1)$ . An unbalanced tensor has  $R_M = \min\{m_T, \prod_{t=1}^{T-1} m_t\}$ , which is similar to matrices. Balanced tensors are expected to have rank  $R_E = \lceil \prod_t m_t / (\sum_t m_t - T + 1) \rceil \leq R_M$  [15, sec. 4] Finding the canonical PD of a tensor is a difficult computational problem. It is possible to find PD with a preset  $R$  (that could be larger or smaller than the actual rank), these are called CANDECOMP/PARAFAC.

Recently, the multiplicative gamma process CANDECOMP/PARAFAC (MGP-CP) [16, 17] was proposed as a statistical model that can infer the rank of a particular tensor in addition to finding the singular values/vectors. The MGP imposes that the singular values should shrink in absolute value as  $r$  increases. The MGP shrinks the variance of a zero mean Gaussian (the prior for  $\lambda_r$ ), so that for large  $r$  the singular value will be near zero with high probability. When a singular value shrinks enough (e.g.,  $\lambda_r < 10^{-6}$ ) we assume it is zero. The numerical rank is given by the number of nonzero  $\lambda_r$  after thresholding. The MGP-CP is described entrywise,  $x_i = \sum_{r=1}^R \lambda_r \prod_{t=1}^T u_{i_t r}^{(t)} + \epsilon_i$  is the  $i^{\text{th}}$  entry of  $\mathcal{X}$ ,  $R$  is the maximum desired rank and  $\epsilon_i$  is Gaussian noise. The MGP-CP is specified as

$$x_i \sim \mathcal{N}\left(\sum_{r=1}^R \lambda_r \prod_{t=1}^T u_{i_t r}^{(t)}, \tau_\epsilon^{-1}\right), \lambda_r \sim \mathcal{N}(0, \tau_{kr}^{-1}), \mathbf{u}_r^{(t)} \sim \mathcal{N}(0, \omega_{rt}^{-1}\mathbf{I}_{n_t}), \tau_{kr} = \prod_{i=1}^r \delta_i, \delta_i \sim \text{Gamma}(\alpha, 1) \quad (2)$$

and  $\tau_\epsilon, \omega_{rt}$  have noninformative gamma priors with all hyperparameters set to  $10^{-6}$ . The shape parameter  $\alpha$  for the MGP is usually set to 2 or 3. If  $\alpha > 1$ , the error in  $\sum_{r=1}^R \lambda_r \prod_{t=1}^T u_{i_t r}^{(t)}$  converges to zero exponentially fast as  $R \rightarrow \infty$  [17]. MGP-CP is also a fully conjugate model and can be implemented as a Gibbs sampler.

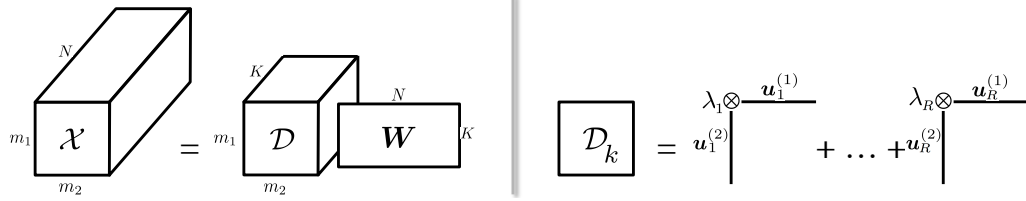


Figure 1: An illustration of the TFA Model for 2-way data. The left equation shows the mode-3 tensor product generalization of dictionary learning. The right equation shows the representation of dictionary atom  $k$  using the MGP-CP, for 2-way data this is the SVD. The illustration clearly shows the reduction in the number of parameters compared to a non-decomposed dictionary. Each atom in a non-decomposed dictionary will have  $\prod m_t$  parameters, while our approach has  $R(1 + \sum m_t)$ . The ability to specify  $R$  gives our model greater flexibility. Moreover, by applying shrinkage on  $\lambda_r$  and learning the expected shrinkage rate  $\alpha$  our model automatically adjusts complexity during learning by finding minimum-rank decompositions of the atoms.

### 3 Tensor Factor Analysis

The most natural generalization of dictionary learning to tensors is to model the data as the product of a dictionary tensor and a weight matrix along the  $(T + 1)^{\text{st}}$  dimension of the dictionary. Although this construction is simple, we have not seen it in the literature. We define the mode- $t$  tensor product  $\times_t$  with an example: the mode-3 product of a tensor  $\mathcal{D} \in \mathbb{R}^{m_1 \times m_2 \times K}$  and a matrix  $\mathbf{W} \in \mathbb{R}^{K \times N}$  yields  $\mathcal{X} = \mathcal{D} \times_3 \mathbf{W} \in \mathbb{R}^{m_1 \times m_2 \times N}$  with  $x_{i_1 i_2 i_3} = \sum_{k=1}^K d_{i_1 i_2 k} w_{k i_3}$ . The factorization is illustrated for 2-way data in figure 1.

We adapt BPFA to the tensor setting by inferring the singular vectors/values of each atom. This is made possible by substituting a MGP-CP decomposition for each atom in the likelihood. It is important to note that during computation we are not replacing the dictionary with a low-rank approximation. The singular vectors/values are drawn from their posteriors. We call this new model tensor-factor analysis (TFA). The model is specified as follows:

$$\begin{aligned}
 \mathcal{X}_n &\sim \mathcal{TN} \left( \mathcal{D} \times_{T+1} (\mathbf{s}_n \circ \mathbf{z}_n), \gamma_\epsilon^{-1} \mathcal{I} \right), & d_{ik} &= \sum_{r=1}^R \lambda_{rk} \prod_{t=1}^T u_{i_t r}^{(kt)}, \\
 u_{i_t r}^{(kt)} &\sim \mathcal{N}(0, \omega_{krt}^{-1}), & \lambda_{kr} &\sim \mathcal{N}(0, \tau_{kr}^{-1}) & \tau_{kr} &= \prod_{i=1}^r \delta_{ki}, & \delta_{ki} &\sim \text{Gamma}(\alpha, 1), \\
 s_{kn} &\sim \mathcal{N}(0, \gamma_s^{-1}), & z_{kn} &\sim \text{Bernoulli}(\pi_k), & \pi_k &\sim \text{Beta}(a_\pi/K, b_\pi(K-1)/K),
 \end{aligned} \tag{3}$$

where  $\mathcal{X}_n$  is the  $n^{\text{th}}$  data item, and  $d_{ik}$  is the  $i = [i_1, \dots, i_T]$  element of the  $k^{\text{th}}$  atom. The hyperparameters for  $\gamma_\epsilon, \gamma_s, \omega_{krt}$  are set to  $10^{-6}$  to give a noninformative prior. We use  $a_\pi = K, b_\pi = N/4$ , to enforce more sparsity than in BPFA since we expect our rank-overcomplete model to be more sparse than an overcomplete model. The MGP shape parameter  $\alpha$  is inferred, this is discussed below. The distribution  $\mathcal{TN}$  is the tensor normal distribution. A tensor is normally distributed if  $\text{vec}(\mathcal{X}) \sim \mathcal{N}(\boldsymbol{\mu}, \boldsymbol{\Sigma})$ , where  $\boldsymbol{\Sigma} = \boldsymbol{\Sigma}_1 \otimes \dots \otimes \boldsymbol{\Sigma}_T$  [18]. Note that the negative log-likelihood is simply  $\|\mathcal{X} - \mathcal{D} \times_{T+1} (\mathbf{S} \circ \mathbf{Z})\|_F^2$ , the atom decompositions impose tensor structure and the priors correspond to regularizers. Our model is fully locally conjugate and can be implemented efficiently as a Gibbs sampler. Our model remains compatible with other priors for the weights (e.g., [11]).

In order to gain intuition about the model, consider the case when we fix  $R = 1$ , a separable dictionary. Every atom  $\mathcal{D}_k$  will be rank 1. Then, each data item is a sum of rank 1 tensors. This is a CANDECOMP/PARAFAC where the rank 1 tensors are selected from a dictionary. The rank of the output tensor is determined by the number of nonzero entries in  $\mathbf{z}_n$  ( $\min\{\text{nnz}(\mathbf{z}_n), R_M\}$ ), which act as singular values. Increasing  $R$  yields:  $\mathcal{X}_n = \sum_{k,r} s_{nk} z_{nk} \lambda_{rk} \otimes_t \mathbf{u}_r^{(kt)}$ , which is a CANDECOMP/PARAFAC with the singular values of each atom scaled by  $s_{nk} z_{nk}$ .

**Learning the shape parameter:** The shape parameter is critical to model quality because it determines the shrinkage rate for the singular values. We found that fixing  $\alpha$  generally produces results worse than the non-tensor models. In the original setting of the MGP-CP, a single tensor is inferred, whereas in our work we infer a set of tensors. Updating  $\alpha$  while the model is learned is important because it adjusts the complexity of the dictionary. Note that a similar approach was

taken in [17], where the rank of the tensor was increased or decreased *ad hoc* depending on whether the singular values are larger than or smaller than preset thresholds. It could be possible to learn a separate  $\alpha_k$  for each  $\mathcal{D}_k$ , but separate shape parameters are not explored in this paper.

Our model extends the MGP by adding a prior for  $\alpha$ . The conjugate prior for a gamma distribution with known rate  $\beta = 1$  is given by  $p(\alpha; a, b) \propto \frac{a^{\alpha-1}}{\Gamma(\alpha)^b}$ , so the posterior distribution is

$$p(\alpha | \{\delta_i^{(k)}\}, a, b) = \text{Gamma}(\delta_{ki}; \alpha, 1) p(\alpha; a, b) \propto \left( a \prod_{k,i} \delta_{ki} \right)^{\alpha-1} \Gamma(\alpha)^{-b-RK}. \quad (4)$$

Although this prior gives straightforward updates, it does not have a closed form. We use numerical integration to perform inverse-CDF sampling. The posterior distribution is strongly peaked and thin-tailed. If  $b$  is small,  $p(\alpha| -)$  is not skewed. Using the *maximum a posteriori* (MAP) solution to update  $\alpha$  also works well and is simpler.

We choose the hyperparameters  $a = b = 10^{-6}$  and set the initial value for  $\alpha = 10^6$ . This causes the model to gradually increase from rank 1 atoms up to the inferred minimal rank. Without sampling  $\alpha$ , the parameters  $R$  and  $\alpha$  must be selected manually. In our approach we set  $R = R_E - 1$  and let the model learn  $\alpha$ . We reduce the rank by 1 to prevent overfitting.

**Scalability:** We use the Bayesian conditional density filter (BCDF) [19] to allow our model to scale to large datasets. Essentially, BCDF allows MCMC models to be trained online or by iterating over subsets of training data. We record surrogate conditional sufficient statistics (SCSS) for the global parameters that directly interact with the data or local parameters  $\mathcal{D}$ ,  $\gamma_\epsilon$ ,  $\gamma_s$ ,  $\pi$ . The SCSS are given by the posterior updates of the global parameters. The SCSS are accumulated for each subset of data, and then applied in the subsequent update as the prior parameters. We reset the SCSS after the number of data items seen is the same as the size of the dataset. In our implementation we update the model parameters 3 times using a single subset of data. The SCSS are held fixed until the 3<sup>rd</sup> iteration. This allows stale local parameters  $\{\mathcal{S}, \mathcal{Z}\}$  to be refreshed before updating the SCSS.

## 4 Deep Convolutional TFA

Instead of matrix-vector multiplication between the atoms and the sparse weights we can use convolution. This will imbue the model with translational invariance; specializing BPFA with a convolutional likelihood is called CFA. In the setting of images we use the 2D (spatial) convolution, and for multi-channel images the convolution is applied separately to each channel. The likelihood for CFA is  $\mathbf{X}_n \sim \mathcal{N}(\sum_k \mathbf{D}_k * \mathbf{W}_{kn}, \gamma_\epsilon^{-1} \mathbf{I}_P)$ , which can be used within the TFA framework by convolving along the  $(T+1)^{\text{st}}$  mode of the dictionary. Note that the weights  $\mathbf{W}_{kn}$  are matrices and the data  $\mathbf{X}_n \in \mathbb{R}^{M_x \times M_y \times M_c}$  and dictionary atoms  $\mathbf{D}_k \in \mathbb{R}^{m_x \times m_y \times M_c}$  are tensors (e.g.,  $M_c = 3$  for RGB images). Usually, the dimensions of the dictionary atoms are much smaller than the image dimensions ( $m_x \ll M_x$  and  $m_y \ll M_y$ ). The spatially-dependent activation weights for dictionary atom  $k$ , image  $n$ , are  $\mathbf{W}_{kn} \in \mathbb{R}^{(M_x - m_x + 1) \times (M_y - m_y + 1)}$ . More details can be found in [20–22]. The dictionary atoms, although they are tensors, are sampled from a multivariate Gaussian. Thus, we can tensorize CFA by introducing the MGP-CP, just as was done in BPFA.

In a deep architecture, the set of weights  $\{\mathbf{W}_{kn}\}_{k=1}^K$  for image  $n$  are represented in terms of (different) convolutional dictionary atoms. When an  $L$ -layer deep model is built, the input of  $\ell^{\text{th}}$  layer is usually composed of a pooled version of the output of the layer below, the  $(\ell-1)^{\text{st}}$  layer. We can formulate this deep deconvolutional model via these two contiguous layers:

$$\mathbf{X}_n^{(\ell-1)} = \sum_{k=1}^{K_{\ell-1}} \mathbf{D}_k^{(\ell-1)} * \mathbf{W}_{kn}^{(\ell-1)}, \quad \mathbf{W}_{kn}^{(\ell-1)} = \text{unpool}(\mathbf{X}_{kn}^{(\ell)}), \quad \mathbf{X}_n^{(\ell)} = \sum_{k=1}^{K_\ell} \mathbf{D}_k^{(\ell)} * \mathbf{W}_{kn}^{(\ell)}. \quad (5)$$

The weights  $\mathbf{W}_{kn}^\ell$  in the  $\ell^{\text{th}}$ -layer become the inputs to the  $(\ell+1)^{\text{st}}$ -layer after pooling. The input tensor  $\mathbf{X}_n^{\ell+1}$  is constituted by stacking the  $K_\ell$  spatially aligned  $\mathbf{X}_{kn}^{\ell+1}$ . The  $(\ell+1)^{\text{st}}$ -layer inputs are tensors with the third-dimension of size  $K_\ell$ , the dictionary size in the  $\ell^{\text{th}}$ -layer. This is deep CFA. When a stochastic unpooling process is employed in (5), and appropriate priors are imposed on dictionary and feature parameters [22], the model developed in (5) constitutes a generative model for images called DGDN.

Within each layer of the deep CFA and DGDN model we employ TFA—convolving along the  $(T+1)^{\text{st}}$  dimension, resulting in deep CTFA and tensor DGDN. A major difference from multiplicative TFA is that both the weights and the dictionary are tensors. The tensor DGDN can also be extended for supervised tasks by connecting a Bayesian SVM [23] to the top layer weights  $W_{kn}^L$  [22].

## 5 Related Work

Rai et al. [17] applied their tensor factorization to the original data tensor. We extracted patches and applied their method to the tensor of patches in the grayscale experiment. The patch-based approach is superior. For example, using BPFA/TFA on non-overlapping  $5 \times 5 \times 5$  patches for 50% inpainting on the amino dataset from [17] gives a 10 trial average MSE of: TFA  $5.6\text{e-}6 \pm 8.0\text{e-}8$ ; BPFA  $1.4\text{e-}5 \pm 2.4\text{e-}6$ . MGP-CP on the original tensor obtains an average MSE of  $5\text{e-}4 \pm 1\text{e-}4$ . Similar results were found for images. However, a patch based approach, as we advocate, gives up the ability to directly infer the rank of the original tensor.

Another difference of TFA and MGP-CP is that TFA infers several tensors simultaneously (the atoms). Because of this we are able to infer a global shrinkage rate  $\alpha$ , which is not possible with a single tensor. Without inferring  $\alpha$  TFA performance suffers. It is also likely that MGP-CP is very sensitive to this parameter. TFA also has significantly less parameters than MGP-CP because the dictionary size is much smaller than the data tensor (the MGP-CP expansion has  $R$  tensors which are the same size as the data tensor).

Some recent work has been done using a separable ( $R = 1$ ) tensor structure for the dictionary. The first approach, separable dictionary learning [7], considered two-way data (grayscale image patches) and claimed generalizing to higher order data was straightforward, but did not show any results in this direction. Their optimization algorithm is significantly more complicated than the separable convolution approach in [6] and for grayscale denoising the performance is not as good as BPFA. The separable multiplicative structure is also considered in [8], where the sample complexity for various dictionary learning approaches is considered.

The paper on learning separable filters [6] considers a convolutional setting, but again separability is enforced. They apply their method to 2- and 3-way data considering denoising and classification. They do not consider a deep generalization. They show that the tensor decomposition can be leveraged to perform faster multiplication, which leads to a sizable reduction in computational complexity. Our model can also benefit from their fast multiplication approach.

## 6 Experiments

In this section we show that maintaining the tensor structure of the data is beneficial in several tasks. We compare against vectorized factor analysis to show that keeping structure can boost performance. All experiments use the default parameters discussed above and none of the parameters were tuned or optimized. We implemented our models in Matlab. All latent parameters are initialized randomly, except  $\alpha$  which is set to  $10^6$  to initialize an essentially separable model.

### 6.1 Image denoising and inpainting

Image denoising is a standard image processing task, and BPFA has been shown to produce very good denoising results without *a priori* knowledge of the noise level [24]. Inpainting is another image processing task, and is a special case of compressive sensing. The goal in the inpainting task is to impute missing pixels.

All of the image processing methods discussed are patch-based. The dataset  $\mathcal{X} \in \mathbb{R}^{B \times B \times C \times N}$  is extracted from the image on a regular grid where the corner of each patch is separated from the other patches by  $(\Delta, \Delta)$  pixels. In these experiments 150 samples are obtained, with the first 40 used as burn-in. The remaining samples are reconstructed as an image, and then averaged to give the final reconstruction. For the CDF-TFA method, we used 10 epochs averaging the last 5 reconstructions, a batch size of 5000 and we update all of the local parameters one time after the first epoch. The time for a single epoch is about 3 times the iteration time for TFA on the full dataset (CDF-TFA has  $3 \times$  more updates). We measure the reconstruction error using the peak signal to noise ratio (PSNR). The grayscale and color image experiments were run on a 2.8 GHz Intel core i7.

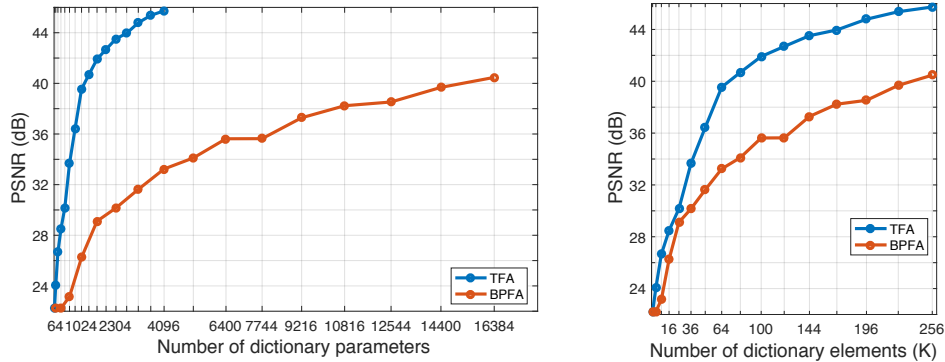


Figure 2: Reconstruction quality for varying model complexity. The same data is plotted with different scalings of the  $x$ -axis: reconstruction PSNR as a function of the number of parameters (left) and as a function of the number of atoms (right).

**Grayscale:** The grayscale experiments use a  $256 \times 256$  Barbara image. The image was chosen so that a direct comparison can be made with published BPFA results. The patch size is  $8 \times 8$  in these experiments.

We first examine the performance of our model by varying the complexity (via dictionary size  $K$ ) of our model and robustness to small sample sizes. The results of the complexity experiment are shown in figure 2; the dictionary size ranges from 1 to 256,  $\Delta = 1$ , and for TFA  $R = 1$ . We see that the tensor based reconstruction with much fewer parameters outperforms BPFA. The number of parameters for the TFA dictionary is  $KR(1 + \sum m_t) = 17K$  and BPFA has  $K \prod m_t = 64K$ . TFA also has a sizable jump in performance just above  $K = R$ , but before  $K = P$ , indicating that rank-overcompleteness is beneficial. For robustness to small sample sizes we train on datasets with  $\Delta = 1, 2, 4, 8$ , corresponding to 100%, 25%, 6.25%, and 1.56% of the patches; results are shown in table 1. We also compare to MGP-CP using the same number of samples as TFA. TFA performs substantially better than BPFA and TFA is more consistent for smaller datasets. We also find the MGP-CP, a tensor method, performs better than BPFA. MGP-CP did not finish the larger datasets in a reasonable amount of time.

Table 1: Reconstruction PSNR (dB) for fractions of the full dataset.

%	100	25	6.25	1.56
TFA	<b>48.43</b>	<b>46.41</b>	<b>46.17</b>	<b>45.04</b>
CDF-TFA	44.56	43.25	40.65	36.46
MGP-CP	—	—	41.01	37.85
BPFA	42.94	40.58	39.20	34.86

Table 2: Reconstruction PSNR (dB) for the Barbara image. Top: TFA, Bottom: BPFA, Subtable: CDF-TFA.

$\sigma$	10%	20%	30%	50%	100%
0	<b>24.24</b>	<b>27.92</b>	<b>30.90</b>	<b>36.03</b>	<b>48.43</b>
	23.47	26.87	29.83	35.60	42.94
5	<b>24.11</b>	<b>27.43</b>	<b>30.08</b>	33.51	<b>38.22</b>
	23.34	26.73	29.27	<b>33.61</b>	37.70
10	<b>23.51</b>	<b>27.18</b>	<b>28.54</b>	<b>31.24</b>	<b>34.44</b>
	23.16	26.07	28.17	31.17	34.31
15	<b>23.09</b>	<b>25.43</b>	<b>27.92</b>	<b>29.36</b>	<b>32.18</b>
	22.66	25.17	26.82	29.31	32.14
20	<b>22.47</b>	<b>24.57</b>	<b>26.09</b>	<b>28.72</b>	<b>30.71</b>
	22.17	24.27	25.62	27.90	30.55
25	<b>21.91</b>	<b>23.96</b>	<b>25.09</b>	<b>27.02</b>	<b>30.17</b>
	21.68	23.49	24.72	26.79	29.30

$\sigma$	0	5	10	15	20
%	10	20	30	50	100
	23.51	26.80	27.92	28.72	30.17

The results for simultaneous denoising and inpainting of the Barbara image are listed in table 2. We find that TFA generally outperforms BPFA. The BPFA results were reported in [24]. The dictionaries learned by each algorithm from the uncorrupted image are shown in figure 3. Qualitatively, the TFA dictionary has a larger variety of structures. The rank (via SVD, with a threshold of  $10^{-6}$ ) of the TFA dictionary atoms ranges between 2 and 7 with 96% having rank 4 or 5. In contrast, every BPFA atom has full rank. TFA dictionaries for  $R = 1, 2, 4, 8$  learned from the uncorrupted image are shown in figure 4. The dictionaries clearly show that TFA can enforce different rank and in the higher rank dictionaries TFA learns low- and high-rank atoms.

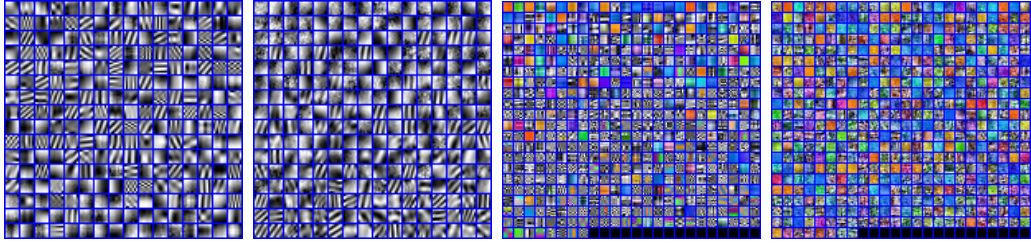


Figure 3: Dictionaries from clean images. Left to right: Barbara TFA, BPFA; Castle TFA, BPFA.

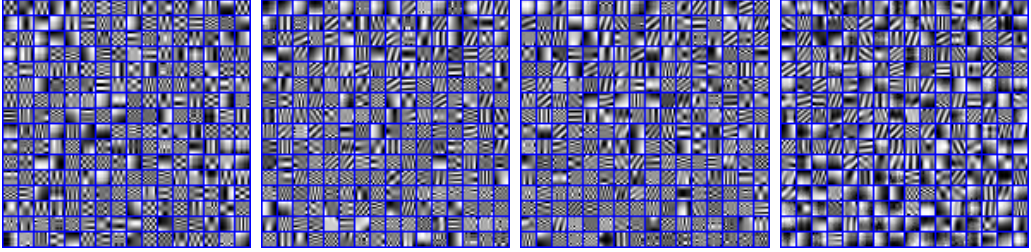


Figure 4: Barbara TFA dictionaries: from left to right  $R = 1, 2, 4, 8$ . For  $R = 1$  TFA learns a very DCT-like dictionary. As the rank increases diagonal structures are added. In the rank 8 dictionary, curved structures are added, but most of the dictionary atoms have rank less than 5.

The results for only inpainting are substantially better than BPFA. TFA gains more than 1 dB in 3 of the cases. For denoising cases TFA also produces superior results. In combined denoising and inpainting TFA performs better than BPFA in all but one case. The average runtime per iteration after burn-in on the uncorrupted Barbara image for both TFA and BPFA is about 13 s. Almost all of the computation time is spent updating the residual, which must be done in both models. The overhead of the the MGP-CP is not noticeable in this experiment.

We noticed that more corrupt data preferred less sparse solutions. For example, with  $b_\pi = 1$  we obtained a PSNR of 24.13 for the case with 10% of the pixels and  $\sigma = 20$ . This setting, however, lead to poor performance for better quality data. This leads us to believe there is a more complex interplay between atom rank, overcompleteness, and sparsity than overcompleteness and sparsity alone.

**Color:** In the color image experiment we use the castle image. The patch size is  $7 \times 7 \times 3$ ,  $\Delta = 1$ , and  $K = 512$ . Denoising and inpainting were performed separately and the reconstruction PSNRs for the castle image are shown in table 3. The inpainting results improve upon BPFA (reported by Zhou et al. [24]), and the denoising results are comparable. We also obtain a PSNR of 50.94 dB on the uncorrupted image using non-overlapping patches. The dictionaries learned by BPFA and TFA are shown in figure 3. Again, the TFA dictionary is more varied. The average runtime per iteration after burn-in on the castle image is: TFA 115 s, BPFA 100 s.

Table 3: Reconstruction PSNR (dB) for the castle image.

PIXEL%	20	30	50	80
TFA	<b>29.58</b>	<b>32.46</b>	<b>37.97</b>	<b>46.62</b>
CDF-TFA	28.95	31.87	37.18	44.60
BPFA	29.12	32.02	36.45	41.51

$\sigma$	5	10	15	25
TFA	<b>40.58</b>	36.20	33.73	30.54
CDF-TFA	39.94	35.63	33.52	30.60
BPFA	40.37	<b>36.24</b>	<b>33.98</b>	<b>31.19</b>

## 6.2 Deep learning

In the next two experiments we test deep CTFA and tensor DGDN. The rank for these experiments was set to  $R = 1$  to minimize training time. Even with such a strong restriction the proposed tensor models outperform the non-tensor models. The hyperparameters for our deep models are set as in [22]; no tuning or optimization was performed.

**Caltech 101:** We resize the images to  $128 \times 128$ , followed by local contrast normalization [25]. The network in this example has 3 layers. The dictionary sizes for each layer are set to  $K_1 = 64$ ,  $K_2 = 125$  and  $K_3 = 128$ , and the dictionary atom sizes are set to  $16 \times 16$ ,  $9 \times 9$  and  $5 \times 5$ . The size of the pooling regions are  $4 \times 4$  (layer 1 to layer 2) and  $2 \times 2$  (layer 2 to layer 3). For classification, we follow the setup in [26], selecting 15 and 30 images per category for training, and up to 50 images per category for testing. The training for the CFA and CTFA models is unsupervised, and the top layer features are used to train an SVM after training the deep model.

Table 4: Caltech 101 classification accuracy (%).

METHOD	15 IMAGES	30 IMAGES
HBP-CFA LAYER-1	53.6	62.5
CTFA LAYER-1	55.7	63.2
DEEP CFA	43.24	53.57
HBP-CFA LAYER-1+2	58.0	65.7
CTFA LAYER-2	57.4	64.5
CTFA LAYER-3	61.2	69.9
DGDN	75.4	87.8
TENSOR DGDN	<b>76.1</b>	<b>88.3</b>

Table 5: MNIST classification error.

METHOD	TEST ERROR %
MCDNN [27]	0.23
6-LAYER CNN [28]	0.35
2-LAYER DGDN [22]	0.37
2-LAYER TENSOR DGDN	0.35

**MNIST:** A two layer model is used with dictionary size  $8 \times 8$  in the first layer and  $6 \times 6$  in the second layer; the pooling size is  $3 \times 3$  and the number of dictionary atoms in layers 1 and 2 are  $K_1 = 36$  and  $K_2 = 152$ . These numbers of dictionary atoms are obtained by setting the initial number of atoms to a relatively large value ( $K_1 = 50$  and  $K_2 = 200$ ), then removing atoms with low usage.

As in the previous deep learning experiment we are comparing the tensor and non-tensor algorithms. The results for MNIST are shown in 5. The state of the art MCDNN is shown as a reference point, MCDNN uses a committee of 35 convnets, elastic distortions, and width normalization. In contrast, we train a single 2-layer model using the original training data. We see that the separable tensor DGDN outperforms DGDN. We also test the robustness of tensor DGDN to small data sets. We compare to the first stochastic pooling work [30] and DGDN. We find the the improvement is consistently better than DGDN.

## 7 Conclusion

We have generalized dictionary learning as a tensor factorization using the  $(T + 1)$ -mode tensor multiplication. Our model need not be separable, which has been the focus of previous work. The MGP-CP tensor decomposition is applied to each dictionary atom to obtain a tensorized BPFA. Moreover, we extend TFA to learn the shrinkage rate for the singular values of each atom. We also show extensions of our approach for online learning and for a deep convolutional setting.

The concept of rank-overcompleteness was also introduced. We showed that rank has a role in the interaction between sparsity and overcompleteness, but the interplay of these three properties requires further study. The performance of TFA and tensor DGDN is promising and has improved state of the art in inpainting and on the Caltech 101 classification benchmark.

We compare to the hierarchical beta process CFA (HBP-CFA) [20], the pretrained DGDN (*i.e.*, deep CFA), and the DGDN [22]. The DGDN models have 3-layers. Other deep CNN models outperform our results in this experiment. However, we are simply showing that using a tensor structured dictionary can improve performance. The results for Caltech 101 are shown in table 4. The one layer CTFA significantly outperforms Deep CFA and is also better than the single layer HBP-CFA. We also find that the 2-layer deep CTFA achieves comparable performance to the deep HBP-CFA using only the top-layer features. The 2-layer HBP-CFA uses both layers of features in the SVM. We also train a 3-layer CTFA and see that the deeper model continues to extract more discriminative features as layers are added. Tensor DGDN provides state of the art accuracy among models *not* pretrained on ImageNet [29].

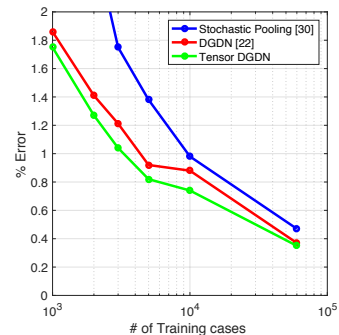


Figure 5: MNIST classification error for varying training data size.

## References

- [1] A. Cichocki, D. Mandic, L. De Lathauwer, G. Zhou, Q. Zhao, C. Caiafa, and H. A. Phan. Tensor decompositions for signal processing applications: From two-way to multiway component analysis. *IEEE Signal Process. Mag.*, 2015.
- [2] L. De Lathauwer, B. De Moor, and J. Vandewalle. A multilinear singular value decomposition. *SIAM J. Matrix Anal. Appl.*, 2000.
- [3] J. Mairal, F. Bach, and J. Ponce. Sparse modeling for image and vision processing. *arXiv:1411.3230*, 2014.
- [4] O. Christensen. *Frames and bases: An introductory course*. Springer, 2008.
- [5] M. S. Lewicki and T. J. Sejnowski. Learning overcomplete representations. *Neural computation*, 2000.
- [6] A. Sironi, B. Tekin, R. Rigamonti, V. Lepetit, and P. Fua. Learning separable filters. *IEEE TPAMI*, 2015.
- [7] S. Hawe, M. Seibert, and M. Kleinsteuber. Separable dictionary learning. In *CVPR*, 2013.
- [8] R. Gribonval, R. Jenatton, F. Bach, M. Kleinsteuber, and M. Seibert. Sample complexity of dictionary learning and other matrix factorizations. *IEEE Trans. Info. Theory*, 2015.
- [9] J. Paisley and L. Carin. Nonparametric factor analysis with beta process priors. In *ICML*, 2009.
- [10] Y. Wang and L. Carin. Levy measure decompositions for the beta and gamma processes. In *ICML*, 2012.
- [11] X. Yuan, V. Rao, S. Han, and L. Carin. Hierarchical infinite divisibility for multiscale shrinkage. *IEEE TSP*, 2014.
- [12] X. Zhang, D. Dunson, and L. Carin. Tree-structured infinite sparse factor model. In *ICML*, 2011.
- [13] Y. Zhang, R. Henao, C. Li, and L. Carin. Bayesian dictionary learning with gaussian processes and sigmoid belief networks. In *IJCAI*, 2016.
- [14] Z. Xing, M. Zhou, A. Castrodad, G. Sapiro, and L. Carin. Dictionary learning for noisy and incomplete hyperspectral images. *SIAM J. Imag. Sci.*, 2012.
- [15] H. Abo, G. Ottaviani, and C. Peterson. Induction for secant varieties of segre varieties. *Transactions of the American Mathematical Society*, 2009.
- [16] A. Bhattacharya and D. Dunson. Sparse Bayesian infinite factor models. *Biometrika*, 2011.
- [17] P. Rai, Y. Wang, S. Guo, G. Chen, D. Dunson, and L. Carin. Scalable bayesian low-rank decomposition of incomplete multiway tensors. In *ICML*, 2014.
- [18] M. Ohlson, M R. Ahmad, and D. Von Rosen. The multilinear normal distribution: Introduction and some basic properties. *Journal of Multivariate Analysis*, 2013.
- [19] Rajarshi Guhaniyogi, Shaan Qamar, and David B Dunson. Bayesian conditional density filtering. *arXiv:1401.3632*, 2014.
- [20] B. Chen, G. Polatkan, G. Sapiro, D. Dunson, and L. Carin. The hierarchical beta process for convolutional factor analysis and deep learning. In *ICML*, 2011.
- [21] Y. Pu, X. Yuan, and L. Carin. Generative deep deconvolutional learning. *arXiv:1412.6039*, 2014.
- [22] Y. Pu, X. Yuan, A. Stevens, C. Li, and L. Carin. A deep generative deconvolutional image model. In *AISTATS*, 2016.
- [23] N. Polson and S. Scott. Data augmentation for support vector machines. *Bayesian Analysis*, 2011.
- [24] M. Zhou, H. Chen, J. Paisley, L. Ren, L. Li, Z. Xing, D. Dunson, G. Sapiro, and L. Carin. Nonparametric Bayesian dictionary learning for analysis of noisy and incomplete images. *IEEE TIP*, 2012.
- [25] K. Jarrett, K. Kavukcuoglu, M. Ranzato, and Y. LeCun. What is the best multi-stage architecture for object recognition? In *ICCV*, 2009.
- [26] J. Yang, K. Yu, Y. Gong, and T. Huang. Linear spatial pyramid matching using sparse coding for image classification. In *CVPR*, 2009.
- [27] D. Ciresan, U. Meier, and J. Schmidhuber. Multi-column deep neural networks for image classification. In *CVPR*, 2012.
- [28] D. Ciresan, J. Meier, U. and Masci, L. Maria Gambardella, and J. Schmidhuber. Flexible, high performance convolutional neural networks for image classification. In *IJCAI*, 2011.
- [29] J. Deng, W. Dong, R. Socher, L. Li, K. Li, and F. Li. Imagenet: A large-scale hierarchical image database. In *CVPR*, 2009.
- [30] M. Zeiler and R. Fergus. Stochastic pooling for regularization of deep convolutional neural networks. In *ICLR*, 2013.